Nonlinear Analysis: Modelling and Control, Online First, 1–18
https://doi.org/10.15388/namc.2025.30.39446

Vilnius University Press

A novel fractional operator-based model for Parkinson's disease: Analyzing abnormal β-oscillation and the influence of synaptic parameters*

Guotao Wang[a,b], **Ningning Huang**[a], **Bashir Ahmad**[c]

[a] Shanxi Key Laboratory of Cryptography and Data Security,
School of Mathematics and Computer Science, Shanxi Normal University,
Taiyuan, Shanxi 030031, China
wgt2512@163.com; hnn0510@163.com

[b] Department of Technical Sciences, Western Caspian University,
Baku 1001, Azerbaijan

[c] Nonlinear Analysis and Applied Mathematics (NAAM) Research Group,
Department of Mathematics, Faculty of Science, King Abdulaziz University,
Jeddah 21589, Saudi Arabia
bashirahmad_qau@yahoo.com

Received: September 26, 2024 / **Revised:** February 14, 2025 / **Published online:** March 12, 2025

Abstract. With the aggravation of the global aging trend, Parkinson's disease has become a hot spot of scientific research all over the world. Abnormal β oscillation in the basal ganglia region is considered to be a major inducement of Parkinson's disease. In this paper, a new and more complete Parkinson's model based on fractional operators is proposed to study the oscillation behavior of the basal ganglia region. The correctness of this new fractional model is validated by the simulation of Nambu and Tachibana's experiment [A. Nambu, Y. Tachibana, Mechanism of parkinsonian neuronal oscillations in the primate basal ganglia: some considerations based on our recent work, *Front. Syst. Neurosci.*, 8:74, 2014]. Then we carry out the Hopf bifurcation analysis of the fractional model and derive the critical conditions for periodic oscillation. The influence of important parameters on the oscillation behavior of the system is analyzed by numerical simulations. It is found that proper control of synaptic transmission delay and synaptic connection strength can improve the abnormal β-oscillation behavior in the basal ganglia region effectively. In addition, the fractional Parkinson's model in this paper provides more flexibility for model fitting and parameter estimation. The choice of the fractional order α plays a crucial role in the analysis of system oscillation.

Keywords: fractional operator-based model for Parkinson's disease, abnormal β-oscillation, Hopf bifurcation, synaptic transmission delay, simulation.

*The work is supported by Natural Science Foundation of Shanxi, China (No. 202403021221163), the Graduate Education Innovation Program of Shanxi, China (No. 2024JG103), and Postgraduate Education Innovation Program of Shanxi Normal University, China(No. 2024YJSKCSZSFK-06).

1 Introduction

Brain science has become the focus of scientific research all over the world in recent years. Among all kinds of brain diseases, Parkinson's disease is a neurodegenerative disease that occurs mostly in middle-aged and elderly people, and it will become more and more serious with age. As the global aging trend intensifies, Parkinson's disease has brought a huge burden to society. Therefore, the pathogenesis and treatment mechanism of Parkinson's disease are always concerned by neuroscience.

Dysfunction of basal ganglia (BG) is considered as the main cause of Parkinson's disease. Basal ganglia is mainly composed of striatum (Str), globus pallidus (GP), subthalamic nucleus (STN), and substantia nigra, which, together with cerebral cortex (Ctx) and thalamus (Th), form the BGTH circuit for controlling motor function. Striatum contains D_1 and D_2 neurons. Globus pallidus can be divided into the inside of globus pallidus (GPi) and the outside of globus pallidus (GPe). Cerebral cortex is divided into two neuronal clusters of excitatory (E) and inhibitory (I). When dopaminergic neurons (D) in the striatum gradually degenerate, the dynamics of neurons in basal nuclei also change. These changes are the core features of Parkinson's disease. It has been found that the neuronal oscillation activity in β frequency band in globus pallidus and hypothalamus is highly correlated with dopaminergic degeneration [10,16]. In order to better explore the mechanism of abnormal β oscillation, researchers have established many mathematical models. Holgado, Terry and Bogacz [12] established a computational model of STN-GPe network, suggesting that β oscillation was caused by STN-GPe loop. However, the experimental results of Nambu and Tachibana [20] showed that Ctx was also important for the oscillation activities of STN and GP. Therefore, Pavlides, Hogan and Bogacz [21] put forward a Ctx-STN-GPe model, which was consistent with the experimental data of Nambu and Tachibana. On the basis of this model, Chen et al. [3] took GPi into account and constructed a Ctx-STN-GPe-GPi model. Liu, Bi and Yang et al. [19] considered the whole BGTH loop and put forward a relatively perfect Ctx-BG-Th model. More research can be found in [5, 9, 11, 17, 18, 24, 29, 30]. It is worth mentioning that mathematical modeling is an effective means to study practical problems and it has a wide range of applications, such as material engineering [8], molecular chemistry [14], bioeconomy [4, 28], and so on. Mathematical modeling also plays an indispensable role in medical research, especially in the field of nervous system diseases.

In recent studies, the Ctx-BG-Th model proposed by Liu et al. [19] did not consider the synaptic transmission delay. Although the Ctx-STN-GPe-GPi model in [3] considered this factor, it did not subdivide the two types of neurons in striatum and ignored the role of thalamus. In addition, the previous studies on abnormal β oscillation in Parkinson's disease were all carried out by establishing integer differential models. No one has developed a fractional differential model yet. Inspired by the above, we build a new and more complete fractional differential model of BGTH loop, which takes into account the synaptic transmission delay and subdivides striatum into D_1 and D_2. Further, we verify the consistency between the new fractional model and the actual experimental results. Through the Hopf bifurcation analysis, it is known that the fractional model will oscillate

periodically. The influence of some important parameters on the oscillation of the new model is studied.

Fractional differential models have unique memorability and heredity, and can describe the time-dependent changes of the system better. In recent decades, they have appeared in more and more scientific fields [1, 2, 6, 7, 13, 22, 25, 26, 31–35]. A fractional differential model usually has more free parameters, which enables researchers to adjust the model more flexibly to match experimental data or clinical observations. These characteristics make the fractional differential model very suitable for the study of Parkinson's disease.

The structure of this paper is as follows: In Section 2, a new fractional BGTH loop differential model is proposed, and the correctness of this fractional model is verified through the simulation of Nambu and Tachibana's experiment. Moreover, the Hopf bifurcation analysis of the new fractional model is carried out. Section 3 analyzes the influence of single parameter and double parameters on oscillation. Section 4 gives the conclusion. The last part is the Appendix.

2 Materials and method

2.1 Fractional BGTH loop differential model

In this part, we establish a new fractional BGTH loop differential model. The fractional model includes Ctx, BG, Th, and their interactions. Among them, BG includes Str, STN, and GP. We divide Str into D_1 and D_2, and GP into GPe and GPi.

E transmits exciting signals to STN, D_1, and D_2 through axons of neurons. STN further transmits the exciting signals to GPe and GPi. GPi outputs inhibitory signals to Th. Th outputs exciting signals to E to form a loop. In addition, E also sends exciting signals to I, and I sends inhibitory signals to E. D_1 and D_2 transmit suppression signals to GPi and GPe, respectively. GPe inputs suppression signals to GPi and STN. We assume that E receive exciting signals of the constant input C. Figure 1 shows the BGTH network described above.

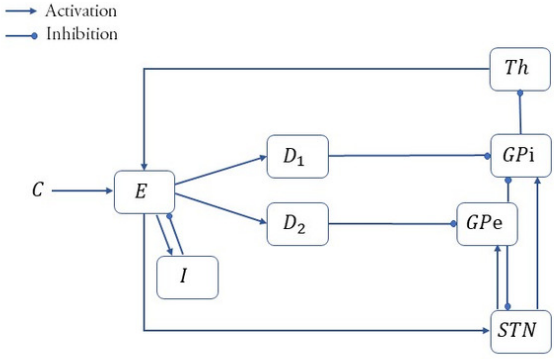

Figure 1. The BGTH network.

For convenience, let the lower corners $i = 1, 2, \ldots, 8$ denote E, I, D_1, D_2, GPe, GPi, Th, STN, respectively. $f_i(t)$ and T_i represent the firing rates of i at time t and the membrane time constants of i, respectively. ω_{ij} represent the connection strength between i and j. τ denotes the synaptic transmission delay. D^α stands for the Caputo fractional derivative of order α, $0 < \alpha \leqslant 1$. The fractional model represented by the network shown in Fig. 1 is as follows:

$$\begin{aligned}
&T_1 D^\alpha f_1(t) = G_1\big(\omega_{71} f_7(t-\tau) - \omega_{21} f_2(t-\tau) + C\big) - f_1(t),\\
&T_2 D^\alpha f_2(t) = G_2\big(\omega_{12} f_1(t-\tau)\big) - f_2(t),\\
&T_3 D^\alpha f_3(t) = G_3\big(\omega_{13} f_1(t-\tau)\big) - f_3(t),\\
&T_4 D^\alpha f_4(t) = G_4\big(\omega_{14} f_1(t-\tau)\big) - f_4(t),\\
&T_5 D^\alpha f_5(t) = G_5\big(\omega_{85} f_8(t-\tau) - \omega_{45} f_4(t-\tau)\big) - f_5(t),\\
&T_6 D^\alpha f_6(t) = G_6\big(\omega_{86} f_8(t-\tau) - \omega_{56} f_5(t-\tau) - \omega_{36} f_3(t-\tau)\big) - f_6(t),\\
&T_7 D^\alpha f_7(t) = G_7\big(-\omega_{67} f_6(t-\tau)\big) - f_7(t),\\
&T_8 D^\alpha f_8(t) = G_8\big(\omega_{18} f_1(t-\tau) - \omega_{58} f_5(t-\tau)\big) - f_8(t).
\end{aligned} \tag{1}$$

G_i represent the activation functions and satisfy the following formula:

$$G_i(in) = \frac{M_i}{1 + (\frac{M_i - B_i}{B_i})\mathrm{e}^{-4in} M_i},$$

where B_i and M_i represent the basic discharge rates and the maximum discharge rates of i, respectively.

2.2 Simulation of the experiment

In this part, we simulate the experiment of Nambu and Tachibana by changing the connection strength in the fractional model and then verify the correctness of our model. The settings of relevant parameters are shown in Table 1. Synaptic transmission delay is 10 ms. More details can be found in [19, 30].

In the experiment, STN was inactivated by injection of muscimol. It was found that the firing rate of GPi decreased and the oscillation weakened. We set $\omega_{86} = 0$ in the model and give Fig. 2 to describe the time history of GPi firing rate. After that, the experiment blocked the glutamatergic input of Ctx to STN and found the oscillation of STN weakened. We set $\omega_{18} = 0$ in the model and give Figs. 3(a), 3(c), and 3(e) to describe the time history of STN firing rate. Finally, researchers blocked the GABAergic input of GPE to STN. They discovered that the firing rate of STN increased, but the oscillation weakened. Let $\omega_{58} = 0$, and Figs. 3(b), 3(d), and 3(f) are given to describe the time history of STN firing rate. As can be seen from the figures, the numerical results of our model are consistent with the experimental results.

Table 1. Parameter values in simulation.

T_i [ms]	Value	B_i [spk/s]	Value	M_i [spk/s]	Value	ω_{ij}	Value	ω_{ij}	Value
T_1	10	B_1	3.62	M_1	71.77	ω_{71}	5	ω_{56}	0.9
T_2	10	B_2	7.18	M_2	276.39	ω_{21}	3.08	ω_{36}	3
T_3	10	B_3	15	M_3	240	ω_{12}	3.08	ω_{67}	5
T_4	10	B_4	15	M_4	240	ω_{13}	5	ω_{18}	6
T_5	14	B_5	75	M_5	400	ω_{14}	5	ω_{58}	6.6
T_6	14	B_6	75	M_6	400	ω_{85}	2.56		
T_7	10	B_7	15	M_7	240	ω_{45}	5		
T_8	6	B_8	17	M_8	300	ω_{86}	2.56		

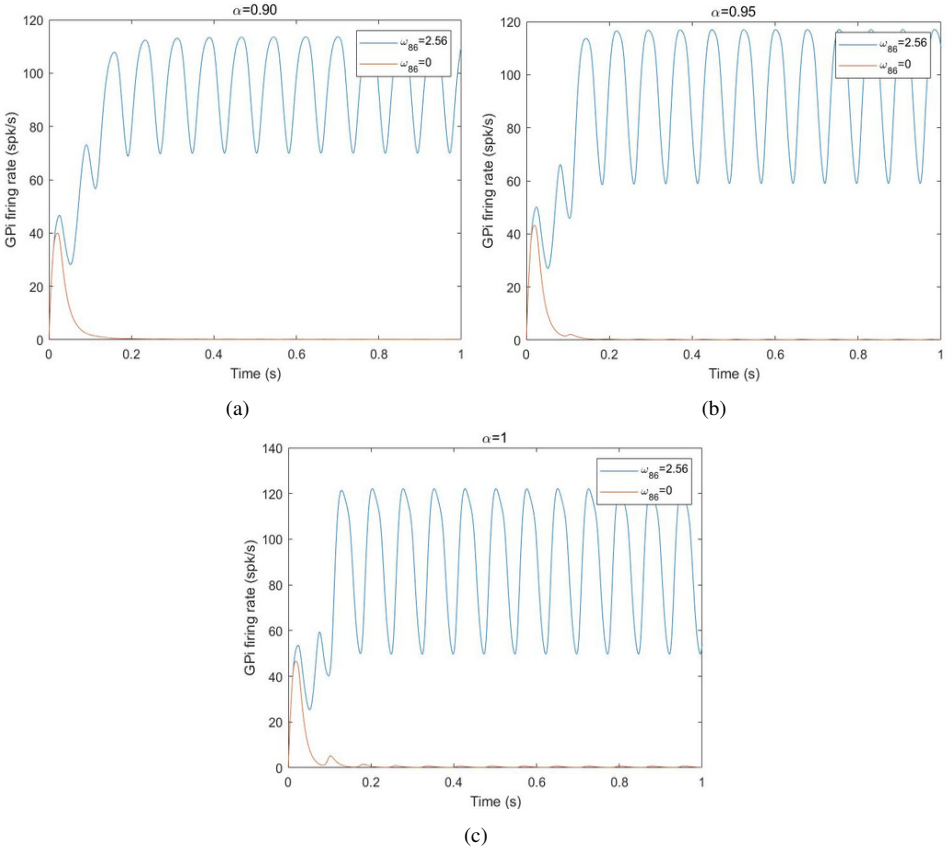

Figure 2. Influence of ω_{86} on the change of GPi firing rate under different fractional orders.

Besides, these figures also manifest that the amplitude of system oscillation varies with the fractional order α. The larger the fractional order α, the greater the amplitude. Therefore, it is helpful for us to study Parkinson's disease more accurately by choosing the appropriate fractional order α according to the actual situation.

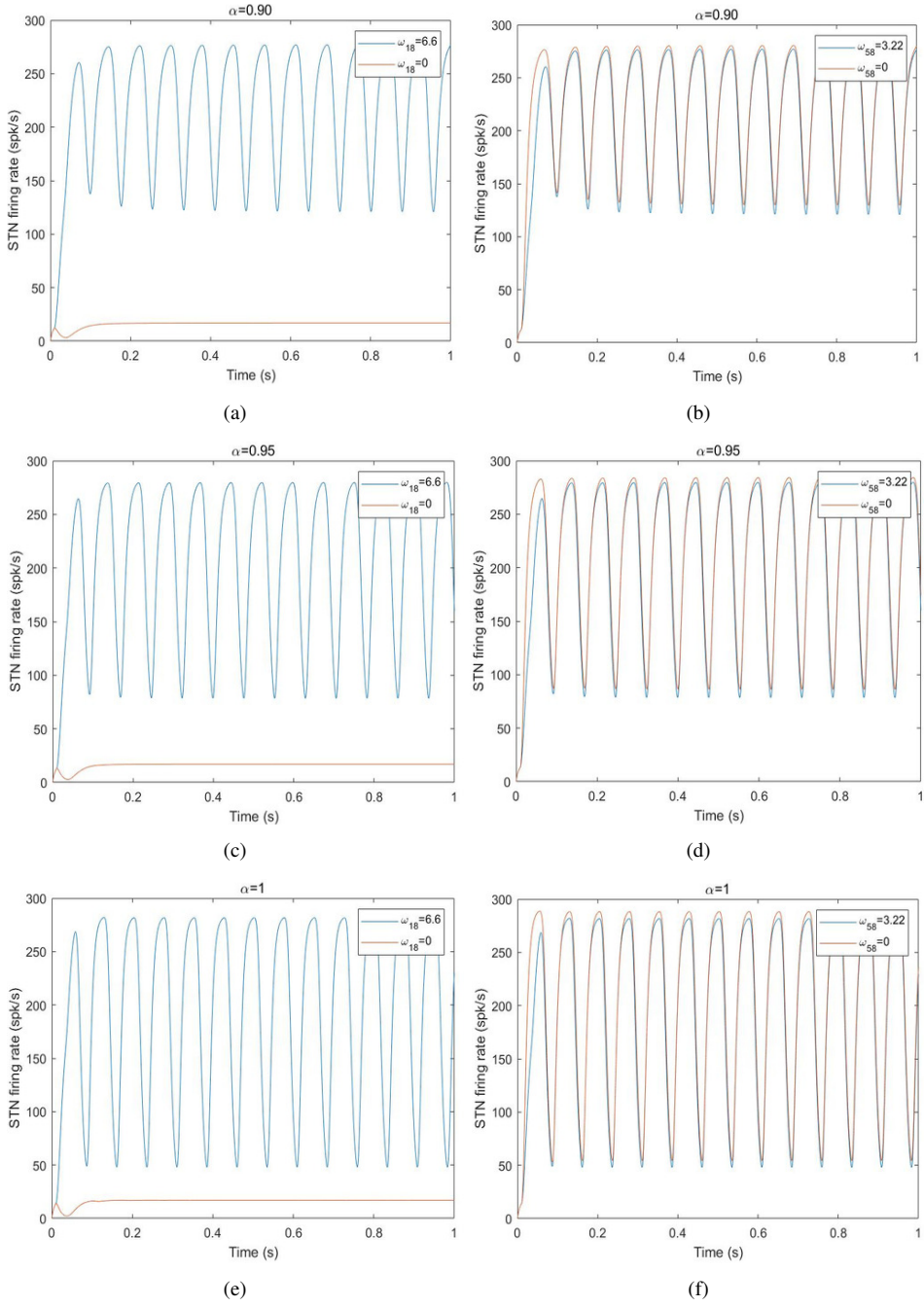

Figure 3. Influence of ω_{18} (a), (c), (e) and ω_{88} (b), (d), (f) on the change of STN firing rate under different fractional orders.

2.3 Hopf bifurcation analysis

In this part, we analyze the Hopf bifurcation of the fractional model (1) and derive the critical conditions for Hopf bifurcation. Related basic theories can be found in [15,23,27].

Because of the complexity of the model, we assume that the membrane time constants are all the same, which is denoted as T. Thus, we can write the fractional model (1) as follows:

$$\begin{aligned}
&TD^{\alpha}f_1(t) = G_1\big(\omega_{71}f_7(t-\tau) - \omega_{21}f_2(t-\tau) + C\big) - f_1(t),\\
&TD^{\alpha}f_2(t) = G_2\big(\omega_{12}f_1(t-\tau)\big) - f_2(t),\\
&TD^{\alpha}f_3(t) = G_3\big(\omega_{13}f_1(t-\tau)\big) - f_3(t),\\
&TD^{\alpha}f_4(t) = G_4\big(\omega_{14}f_1(t-\tau)\big) - f_4(t),\\
&TD^{\alpha}f_5(t) = G_5\big(\omega_{85}f_8(t-\tau) - \omega_{45}f_4(t-\tau)\big) - f_5(t),\\
&TD^{\alpha}f_6(t) = G_6\big(\omega_{86}f_8(t-\tau) - \omega_{56}f_5(t-\tau) - \omega_{36}f_3(t-\tau)\big) - f_6(t),\\
&TD^{\alpha}f_7(t) = G_7\big(-\omega_{67}f_6(t-\tau)\big) - f_7(t),\\
&TD^{\alpha}f_8(t) = G_8\big(\omega_{18}f_1(t-\tau) - \omega_{58}f_5(t-\tau)\big) - f_8(t).
\end{aligned} \tag{2}$$

The nonzero equilibrium point of system (2) is $E^* = (f_1^*, f_2^*, \ldots, f_8^*)$. By substituting $\overline{f}_i = f_i - f_i^*$, system (2) at the equilibrium point E^* can be linearized to

$$D^{\alpha}v(t) = A_1v(t) + A_2v(t-\tau), \tag{3}$$

where $v(t) = (f_1 - f_1^*,\ f_2 - f_2^*,\ \ldots,\ f_8 - f_8^*)^{\mathrm{T}}$,

$$A_1 = \begin{pmatrix}
-\frac{1}{T} & & & & & & & \\
& -\frac{1}{T} & & & & & & \\
& & -\frac{1}{T} & & & & & \\
& & & -\frac{1}{T} & & & & \\
& & & & -\frac{1}{T} & & & \\
& & & & & -\frac{1}{T} & & \\
& & & & & & -\frac{1}{T} & \\
& & & & & & & -\frac{1}{T}
\end{pmatrix},$$

$$A_2 = \begin{pmatrix}
0 & -a_{12} & 0 & 0 & 0 & 0 & a_{17} & 0\\
a_{21} & 0 & 0 & 0 & 0 & 0 & 0 & 0\\
a_{31} & 0 & 0 & 0 & 0 & 0 & 0 & 0\\
a_{41} & 0 & 0 & 0 & 0 & 0 & 0 & 0\\
0 & 0 & 0 & -a_{54} & 0 & 0 & 0 & a_{58}\\
0 & 0 & -a_{63} & 0 & -a_{65} & 0 & 0 & a_{68}\\
0 & 0 & 0 & 0 & 0 & -a_{76} & 0 & 0\\
a_{81} & 0 & 0 & 0 & -a_{85} & 0 & 0 & 0
\end{pmatrix},$$

$$
\begin{aligned}
a_{12} &= \frac{4\omega_{21}f_1^*}{TM_1} - \frac{4\omega_{21}(f_1^*)^2}{TM_1^2}, & a_{17} &= \frac{4\omega_{71}f_1^*}{TM_1} - \frac{4\omega_{71}(f_1^*)^2}{TM_1^2},\\
a_{21} &= \frac{4\omega_{12}f_2^*}{TM_2} - \frac{4\omega_{12}(f_2^*)^2}{TM_2^2}, & a_{31} &= \frac{4\omega_{13}f_3^*}{TM_3} - \frac{4\omega_{13}(f_3^*)^2}{TM_3^2},\\
a_{41} &= \frac{4\omega_{14}f_4^*}{TM_4} - \frac{4\omega_{14}(f_4^*)^2}{TM_4^2}, & a_{54} &= \frac{4\omega_{45}f_5^*}{TM_5} - \frac{4\omega_{45}(f_5^*)^2}{TM_5^2},\\
a_{58} &= \frac{4\omega_{85}f_5^*}{TM_5} - \frac{4\omega_{85}(f_5^*)^2}{TM_5^2}, & a_{63} &= \frac{4\omega_{36}f_6^*}{TM_6} - \frac{4\omega_{36}(f_6^*)^2}{TM_6^2},\\
a_{65} &= \frac{4\omega_{56}f_6^*}{TM_6} - \frac{4\omega_{56}(f_6^*)^2}{TM_6^2}, & a_{68} &= \frac{4\omega_{86}f_6^*}{TM_6} - \frac{4\omega_{86}(f_6^*)^2}{TM_6^2},\\
a_{76} &= \frac{4\omega_{67}f_7^*}{TM_7} - \frac{4\omega_{76}(f_7^*)^2}{TM_7^2}, & a_{81} &= \frac{4\omega_{18}f_8^*}{TM_8} - \frac{4\omega_{81}(f_8^*)^2}{TM_8^2},\\
a_{85} &= \frac{4\omega_{58}f_8^*}{TM_8} - \frac{4\omega_{85}(f_8^*)^2}{TM_8^2}.
\end{aligned}
$$

When $\tau = 0$, the coefficient matrix of the linearized system (3) is $\Lambda = A_1 + A_2$. Then the characteristic equation of Λ is

$$
\begin{aligned}
|\lambda I - \Lambda| &= \begin{vmatrix}
\lambda + \frac{1}{T} & a_{12} & 0 & 0 & 0 & 0 & -a_{17} & 0\\
-a_{21} & \lambda + \frac{1}{T} & 0 & 0 & 0 & 0 & 0 & 0\\
-a_{31} & 0 & \lambda + \frac{1}{T} & 0 & 0 & 0 & 0 & 0\\
-a_{41} & 0 & 0 & \lambda + \frac{1}{T} & 0 & 0 & 0 & 0\\
0 & 0 & 0 & a_{54} & \lambda + \frac{1}{T} & 0 & 0 & -a_{58}\\
0 & 0 & a_{63} & 0 & a_{65} & \lambda + \frac{1}{T} & 0 & -a_{68}\\
0 & 0 & 0 & 0 & 0 & a_{76} & \lambda + \frac{1}{T} & 0\\
-a_{81} & 0 & 0 & 0 & a_{85} & 0 & 0 & \lambda + \frac{1}{T}
\end{vmatrix}\\
&= \lambda^8 + b_1\lambda^7 + b_2\lambda^6 + b_3\lambda^5 + b_4\lambda^4 + b_5\lambda^3 + b_6\lambda^2 + b_7\lambda + b_8 = 0.
\end{aligned}
$$

The specific formulae of b_i are shown in the Appendix. We give the following assumption:

(A_1) $b_i > 0,\ \Delta_i > 0$, where

$$
\Delta_i = \begin{vmatrix}
b_1 & b_3 & b_5 & \cdots & b_{2i-1}\\
b_0 & b_2 & b_4 & \cdots & b_{2i-2}\\
0 & b_1 & b_3 & \cdots & b_{2i-3}\\
\vdots & \vdots & \vdots & \ddots & \vdots\\
0 & 0 & 0 & \cdots & b_i
\end{vmatrix}, \quad i = 1, 2, \ldots, 8.
$$

Then a lemma can be obtained from the Routh–Hurwitz criterion.

Lemma 1. *If* (A_1) *holds, all eigenvalues of the coefficient matrix* Λ *of system* (3) *with* $\tau = 0$ *satisfy* $|\arg(\lambda_i)| > q\pi/2$, $0 < q \leqslant 1$.

Next, we prove that the characteristic equation of system (3) with $\tau = \tau_0$ has a pair of purely imaginary roots $\pm \mathrm{i}w_0$. From [27] the characteristic equation of system (3) is $|s^\alpha I - A_1 - A_2 \mathrm{e}^{-s\tau}| = 0$, that is,

$$C_1(s) + C_2(s)\mathrm{e}^{-2s\tau} + C_3(s)\mathrm{e}^{-4s\tau} + C_4(s)\mathrm{e}^{-5s\tau} = 0, \tag{4}$$

where

$$\begin{aligned}
C_1(s) &= s^{8\alpha} + \beta_1 s^{7\alpha} + \beta_2 s^{6\alpha} + \beta_3 s^{5\alpha} + \beta_4 s^{4\alpha} + \beta_5 s^{3\alpha} + \beta_6 s^{2\alpha} + \beta_7 s^{\alpha} + \beta_8,\\
C_2(s) &= \beta_9 s^{6\alpha} + \beta_{10} s^{5\alpha} + \beta_{11} s^{4\alpha} + \beta_{12} s^{3\alpha} + \beta_{13} s^{2\alpha} + \beta_{14} s^{\alpha} + \beta_{15},\\
C_3(s) &= \beta_{16} s^{4\alpha} + \beta_{17} s^{3\alpha} + \beta_{18} s^{2\alpha} + \beta_{19} s^{\alpha} + \beta_{20},\\
C_4(s) &= \beta_{21} s^{3\alpha} + \beta_{22} s^{2\alpha} + \beta_{23} s^{\alpha} + \beta_{24}.
\end{aligned}$$

The specific formulae of β_i are shown in the Appendix. We rewrite (4) as

$$C_1(s)\mathrm{e}^{2s\tau} + C_2(s) + C_3(s)\mathrm{e}^{-2s\tau} + C_4(s)\mathrm{e}^{-3s\tau} = 0. \tag{5}$$

Suppose that $s = \mathrm{i}w = w(\cos(\pi/2) + \mathrm{i}\sin(\pi/2)$ is the solution of Eq. (5). C_{lR} and C_{lI} are the real part and imaginary part of $C_l(s)$ $(l = 1, 2, 3, 4)$, respectively. Through calculation, we can get

$$\begin{aligned}
C_{1R} &= d_1 w^{8\alpha} + d_2 w^{7\alpha} + d_3 w^{6\alpha} + d_4 w^{5\alpha} + d_5 w^{4\alpha} + d_6 w^{3\alpha} + d_7 w^{2\alpha} + d_8 w^{\alpha} + d_9,\\
C_{1I} &= d_{10} w^{8\alpha} + d_{11} w^{7\alpha} + d_{12} w^{6\alpha} + d_{13} w^{5\alpha} + d_{14} w^{4\alpha} + d_{15} w^{3\alpha} + d_{16} w^{2\alpha} + d_{17} w^{\alpha},\\
C_{2R} &= d_{18} w^{6\alpha} + d_{19} w^{5\alpha} + d_{20} w^{4\alpha} + d_{21} w^{3\alpha} + d_{22} w^{2\alpha} + d_{23} w^{\alpha} + d_{24},\\
C_{2I} &= d_{25} w^{6\alpha} + d_{26} w^{5\alpha} + d_{27} w^{4\alpha} + d_{28} w^{3\alpha} + d_{29} w^{2\alpha} + d_{30} w^{\alpha},\\
C_{3R} &= d_{31} w^{4\alpha} + d_{32} w^{3\alpha} + d_{33} w^{2\alpha} + d_{34} w^{\alpha} + d_{35},\\
C_{3I} &= d_{36} w^{4\alpha} + d_{37} w^{3\alpha} + d_{38} w^{2\alpha} + d_{39} w^{\alpha},\\
C_{4R} &= d_{40} w^{3\alpha} + d_{41} w^{2\alpha} + d_{42} w^{\alpha} + d_{43},\\
C_{4I} &= d_{44} w^{3\alpha} + d_{45} w^{2\alpha} + d_{46} w^{\alpha}.
\end{aligned}$$

The specific formulae of d_i are shown in the Appendix. Substituting the solution into (5) and distinguishing the real part from the imaginary part, one has

$$\begin{aligned}
&(C_{1R} + \mathrm{i}C_{1I})(\cos 2w\tau + \mathrm{i}\sin 2w\tau) + (C_{2R} + \mathrm{i}C_{2I})\\
&\quad + (C_{3R} + \mathrm{i}C_{3I})(\cos 2w\tau - \mathrm{i}\sin 2w\tau)\\
&\quad + (C_{4R} + iC_{4I})(\cos 3w\tau - i\sin 3w\tau) = 0.
\end{aligned}$$

It follows from the above that

$$\begin{aligned}
&(C_{1R} + C_{3R})\cos 2w\tau + (C_{3I} - C_{1I})\sin 2w\tau + C_{2R}\\
&\quad = -C_{4I}\sin 3w\tau - C_{4R}\cos 3w\tau,\\
&(C_{1I} + C_{3I})\cos 2w\tau + (C_{1R} - C_{3R})\sin 2w\tau + C_{2I}\\
&\quad = C_{4R}\sin 3w\tau - C_{4I}\cos 3w\tau.
\end{aligned} \tag{6}$$

Let

$$F_1 = C_{1R} + C_{3R}, \qquad F_2 = C_{3I} - C_{1I},$$
$$F_3 = C_{1I} + C_{3I}, \qquad F_4 = C_{1R} - C_{3R},$$

the following can be obtained from (6):

$$\begin{aligned}&\left(F_1^2 + F_3^2\right)\cos^2 2w\tau + \left(F_2^2 + F_4^2\right)\sin^2 2w\tau + 2(F_1C_{2R} + F_3C_{2I})\cos 2w\tau \\ &\quad + 2(F_2C_{2R} + F_4C_{2I})\sin 2w\tau + 2(F_1F_2 + F_3F_4)\sin 2w\tau\cos 2w\tau \\ &= \left(C_{4I}^2 + C_{4R}^2\right)^2 - C_{2R}^2 - C_{2I}^2.\end{aligned}$$

It is equivalent to

$$\begin{aligned}&\cos^4 2w\tau + \frac{2(ac - bc + de)}{a^2 + b^2 + \mathrm{e}^2 - 2ab}\cos^3 2w\tau \\ &\quad + \frac{c^2 + d^2 - \mathrm{e}^2 + 2(ab - am + bm - b^2)}{a^2 + b^2 + \mathrm{e}^2 - 2ab}\cos^2 2w\tau \\ &\quad - \frac{2(de + cm - bc)}{a^2 + b^2 + \mathrm{e}^2 - 2ab}\cos 2w\tau - \frac{d^2 - b^2 - m^2 + 2bm}{a^2 + b^2 + \mathrm{e}^2 - 2ab} = 0,\end{aligned} \tag{7}$$

where

$$a = F_1^2 + F_3^2, \qquad c = 2(F_1C_{2R} + F_3C_{2I}), \qquad e = 2(F_1F_2 + F_3F_4),$$
$$b = F_2^2 + F_4^2, \qquad d = 2(F_2C_{2R} + F_4C_{2I}), \qquad m = \left(C_{4I}^2 + C_{4R}^2\right)^2 - C_{2R}^2 - C_{2I}^2.$$

Let us denote

$$G_1 = \frac{2(ac - bc + de)}{a^2 + b^2 + \mathrm{e}^2 - 2ab}, \qquad G_2 = \frac{c^2 + d^2 - \mathrm{e}^2 + 2(ab - am + bm - b^2)}{a^2 + b^2 + \mathrm{e}^2 - 2ab},$$
$$G_3 = -\frac{2(de + cm - bc)}{a^2 + b^2 + \mathrm{e}^2 - 2ab}, \qquad G_4 = -\frac{d^2 - b^2 - m^2 + 2bm}{a^2 + b^2 + \mathrm{e}^2 - 2ab}.$$

Then Eq. (7) implies that

$$\cos^4 2w\tau + G_1\cos^3 2w\tau + G_2\cos^2 2w\tau + G_3\cos 2w\tau + G_4 = 0. \tag{8}$$

In order to get the theoretical results, we need the following assumption:

(A_2) $(1 + G_2 + G_4)^2 \leqslant (G_1 + G_3)^2$.

According to the zero theorem, there is at least one solution of (8), which is denoted as ρ_i ($i \leqslant 4$, $i \in \mathbb{N}^+$). Consequently,

$$\tau_i^{(k)} = \frac{1}{2w_i}(\arccos\rho_i + 2k\pi), \quad k = 0, 1, 2, \ldots .$$

Let $\tau_0 = \min\{\tau_i^{(k)}\}$. When $\tau = \tau_0$, we have $w = w_0$. It is concluded that Eq. (4) has a pair of purely imaginary roots $\pm \mathrm{i}w_0$ when $\tau = \tau_0$.

Finally, $\mathrm{Re}[\mathrm{d}s(\tau)/\mathrm{d}\tau]|_{\tau=\tau_0,\, w=w_0} > 0$ can be verified. Taking the derivative of τ on both sides of (5), one can get that

$$\frac{\mathrm{d}s}{\mathrm{d}\tau} = \frac{X(s)}{Y(s)},$$

where

$$\begin{aligned} X(s) &= 3sC_4(s)\mathrm{e}^{-3s\tau} + 2sC_3(s)\mathrm{e}^{-2s\tau} - 2sC_1(s)\mathrm{e}^{2s\tau}, \\ Y(s) &= \big(C_4'(s) - 3\tau C_4(s)\big)\mathrm{e}^{-3s\tau} + \big(C_3'(s) - 2\tau C_3(s)\big)\mathrm{e}^{-2s\tau} \\ &\quad + \big(2\tau C_1(s) + C_1'(s)\big)\mathrm{e}^{2s\tau} + C_2'(s). \end{aligned}$$

Separate the real part and imaginary part of $X(s)$ and $Y(s)$ to obtain

$$X(s) = X_1 + \mathrm{i}X_2, \qquad Y(s) = Y_1 + \mathrm{i}Y_2.$$

Further,

$$\mathrm{Re}\left[\frac{\mathrm{d}s(\tau)}{\mathrm{d}\tau}\right] = \frac{X_1Y_1 + X_2Y_2}{Y_1^2 + Y_2^2}.$$

Let the following hypothesis hold:

(A_3) $(X_1Y_1 + X_2Y_2)/(Y_1^2 + Y_2^2)|_{\tau=\tau_0,\, w=w_0} > 0.$

Then we have

$$\mathrm{Re}\left[\frac{\mathrm{d}s(\tau)}{\mathrm{d}\tau}\right]\Bigg|_{\tau=\tau_0, w=w_0} > 0.$$

Taking all the above into account, we can arrive at the conclusion of this section.

Theorem 1. *Under* (A_1)–(A_3)*, system* (2) *experiences Hopf bifurcation at the equilibrium point* $E^* = (f_1^*, f_2^*, \ldots, f_8^*)$.

3 Results and discussion

In this section, we employ numerical simulations to analyze the influence of related parameters on abnormal β oscillation. Except for the variable parameters, the values of other parameters refer to Section 2.2. We take the fractional order α as 0.95.

The effect of single parameter is analyzed first. Figure 4 displays the influence of synaptic connection strength of D_1 and GPi on GPi oscillation. It can be found from Fig. 4(a) that with the increase of ω_{36}, the firing rate of GPi decreases, but the amplitude increases. To further explore the influence of ω_{36} on GPi oscillation, we continue to increase the value of ω_{36}. The result from Fig. 4(b) displays that with the increase of ω_{36}, the discharge rate and amplitude of GPi both decrease gradually. In other words, when the value of ω_{36} is within a certain range, the oscillation of GPi exacerbates with the increase of ω_{36}. But GPi will return to a stable state when ω_{36} is large enough.

Next, the effect of double parameters is analyzed. Figure 5(a) shows the effects of ω_{36} and ω_{56} on the GPi amplitude. Figure 5(b) shows the effects of ω_{36} and ω_{86} on the GPi

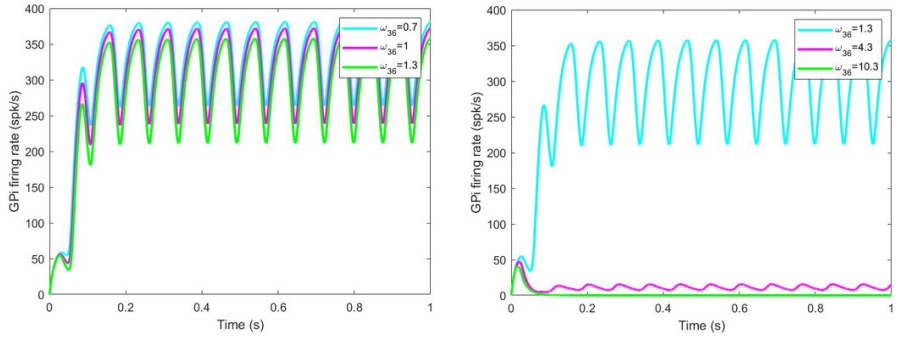

(a) (b)

Figure 4. Influence of ω_{36} on the oscillation of GPi. (a) Variation of GPi firing rate over time when ω_{36} takes 0.7, 1, and 1.3, respectively. (b) Variation of GPi firing rate over time when ω_{36} takes 1.3, 4.3, and 10.3, respectively.

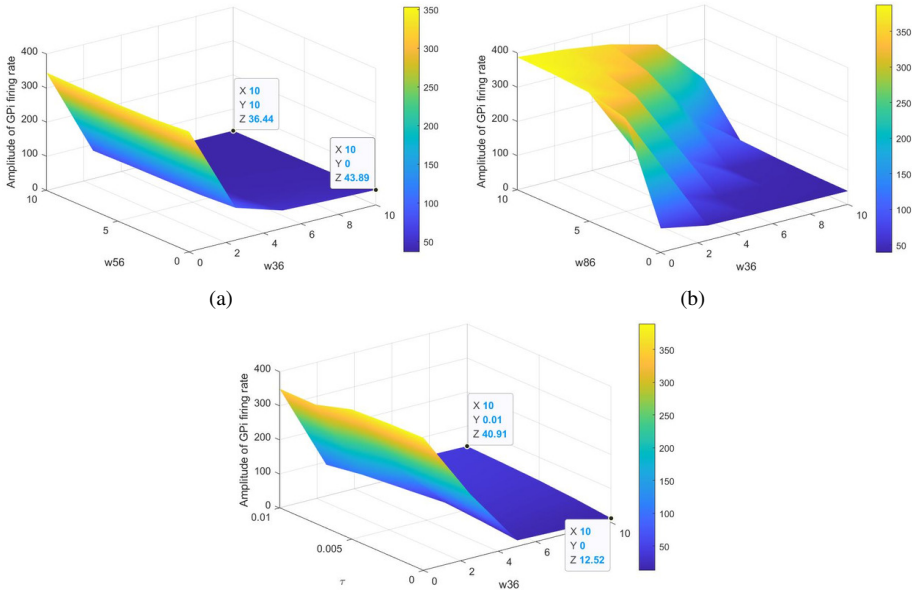

(a) (b)

(c)

Figure 5. Influence of double parameters on the amplitude of GPi. (a) Influence of ω_{36} and ω_{56} on the amplitude of GPi. (b) Influence of ω_{36} and ω_{86} on the amplitude of GPi. (c) Influence of ω_{36} and τ on the amplitude of GPi.

amplitude. Figure 5(c) shows the effects of ω_{36} and τ on the GPi amplitude. It can be seen that the amplitude of GPi diminishes gradually, while ω_{36} and ω_{56} rise simultaneously. When ω_{36} and ω_{86} take the maximum and minimum values, respectively, the amplitude of GPi is the smallest. With the increase of ω_{36} and the decrease of τ, the amplitude of GPi will decrease gradually.

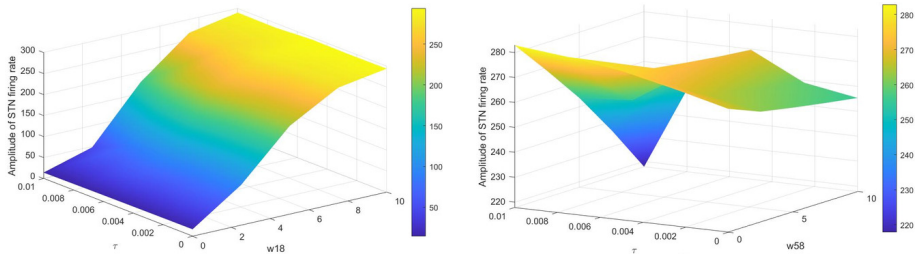

(a) (b)

Figure 6. Influence of double parameters on the amplitude of STN. (a) Influence of ω_{18} and τ on the amplitude of STN. (b) Influence of ω_{58} and τ on the amplitude of STN.

Figure 6 exhibits the influence of two parameters on the amplitude of STN. In Fig. 6(a), the oscillation of STN wanes with the raise of τ and the reduction of ω_{18}. In Fig. 6(b), when τ and ω_{58} are both maximum, the amplitude of STN is minimum.

4 Conclusion

The pathogenesis of Parkinson's disease is extremely complicated, and it is still not fully understood as yet. However, the abnormal β oscillation in basal ganglia has been proved to be closely related to Parkinson's disease. In order to further explore the etiology and treatment of Parkinson's disease, this paper proposed a new fractional BGTH loop model with time delay based on integer-order Parkinson's models in previous research. Through the simulation of Nambu and Tachibana's experiment, we validated the correctness of the new fractional model. Then we performed Hopf bifurcation analysis on the new fractional model and proved the existence of the Hopf bifurcation point, which showed that the system would produce periodic oscillation with the increase of time delay. Finally, the important influence of related parameters on the system state was verified through numerical simulations.

In addition, the fractional BGTH loop differential model in this paper provides more flexibility for model fitting and parameter estimation. From the simulation of the experiment in Section 2 we can see that the choice of the fractional order α also plays an important role in the analysis of system oscillation. It is hoped that the results of this paper can provide a deeper understanding for the study of Parkinson's disease.

Appendix

Specific formulae not given in Section 2.3 will be presented in this section.

$$b_1 = \frac{8}{T}, \qquad b_2 = a_{12}a_{21} + a_{58}a_{85} + \frac{28}{T^2},$$
$$b_3 = \frac{6a_{58}a_{85} + 6a_{12}a_{21}}{T} + \frac{56}{T^3},$$

$$
\begin{aligned}
b_4 &= a_{17}a_{68}a_{76}a_{81} - a_{17}a_{31}a_{63}a_{76} \\
&\quad + \frac{a_{12}a_{21}a_{58}a_{85} + 15a_{12}a_{21} + 15a_{58}a_{85}}{T^2} + \frac{70}{T^4}, \\
b_5 &= a_{17}a_{41}a_{54}a_{65}a_{76} - a_{17}a_{58}a_{65}a_{76}a_{81} \\
&\quad + \frac{4a_{17}a_{68}a_{76}a_{81} + 4a_{12}a_{21}a_{58}a_{85} - 4a_{17}a_{31}a_{63}a_{76}}{T} \\
&\quad + \frac{20a_{58}a_{85} + 20a_{12}a_{21}}{T^3} + \frac{56}{T^5}, \\
b_6 &= a_{17}a_{41}a_{54}a_{68}a_{76}a_{85} - a_{17}a_{31}a_{58}a_{63}a_{76}a_{85} \\
&\quad + \frac{3a_{17}a_{41}a_{54}a_{65}a_{76} - 3a_{17}a_{58}a_{65}a_{76}a_{81}}{T} \\
&\quad + \frac{6a_{12}a_{21}a_{58}a_{85} + 6a_{17}a_{68}a_{76}a_{81} - 6a_{17}a_{31}a_{63}a_{76}}{T^2} \\
&\quad + \frac{15a_{12}a_{21} + 15a_{58}a_{85}}{T^4} + \frac{28}{T^6}, \\
b_7 &= \frac{2a_{17}a_{41}a_{54}a_{68}a_{76}a_{85} - 2a_{17}a_{31}a_{58}a_{63}a_{76}a_{85}}{T} \\
&\quad + \frac{3a_{17}a_{41}a_{54}a_{65}a_{76} - 3a_{17}a_{58}a_{65}a_{76}a_{81}}{T^2} \\
&\quad + \frac{4a_{12}a_{21}a_{58}a_{85} - 4a_{17}a_{31}a_{63}a_{76} + 4a_{17}a_{68}a_{76}a_{81}}{T^3} \\
&\quad + \frac{6a_{12}a_{21} + 6a_{58}a_{85}}{T^5} + \frac{8}{T^7}, \\
b_8 &= \frac{a_{17}a_{41}a_{54}a_{68}a_{76}a_{85} - a_{17}a_{31}a_{58}a_{63}a_{76}a_{85}}{T^2} \\
&\quad + \frac{a_{17}a_{41}a_{54}a_{65}a_{76} - a_{17}a_{58}a_{65}a_{76}a_{81}}{T^3} \\
&\quad + \frac{a_{12}a_{21}a_{58}a_{85} + a_{17}a_{68}a_{76}a_{81} - a_{17}a_{31}a_{63}a_{76}}{T^4} \\
&\quad + \frac{a_{12}a_{21} + a_{58}a_{85}}{T^6} + \frac{1}{T^8};
\end{aligned}
$$

$$
\begin{aligned}
&\beta_1 = \frac{8}{T}, \quad \beta_2 = \frac{28}{T^2}, \quad \beta_3 = \frac{56}{T^3}, \quad \beta_4 = \frac{70}{T^4}, \quad \beta_5 = \frac{56}{T^5}, \\
&\beta_6 = a_{17}a_{41}a_{54}a_{68}a_{76}a_{85} - a_{17}a_{31}a_{58}a_{63}a_{76}a_{85} + \frac{28}{T^6}, \\
&\beta_7 = \frac{2a_{17}a_{41}a_{54}a_{68}a_{76}a_{85} - 2a_{17}a_{31}a_{58}a_{63}a_{76}a_{85}}{T} + \frac{8}{T^7}, \\
&\beta_8 = \frac{a_{17}a_{41}a_{54}a_{68}a_{76}a_{85} - a_{17}a_{31}a_{58}a_{63}a_{76}a_{85}}{T^2} + \frac{1}{T^8}, \\
&\beta_9 = a_{58}a_{85} + a_{12}a_{21}, \quad \beta_{10} = \frac{6a_{58}a_{85} + 6a_{12}a_{21}}{T}, \\
&\beta_{11} = \frac{15a_{12}a_{21} + 15a_{58}a_{85}}{T^2}, \quad \beta_{12} = \frac{20a_{12}a_{21} + 20a_{58}a_{85}}{T^3},
\end{aligned}
$$

$$\beta_{13} = \frac{15a_{58}a_{85} + 15a_{12}a_{21}}{T^4}, \qquad \beta_{14} = \frac{6a_{12}a_{21} + 6a_{58}a_{85}}{T^5},$$
$$\beta_{15} = \frac{a_{12}a_{21} + a_{58}a_{85}}{T^6},$$
$$\beta_{16} = a_{12}a_{21}a_{58}a_{85} + a_{17}a_{68}a_{76}a_{81} - a_{17}a_{31}a_{63}a_{76},$$
$$\beta_{17} = \frac{4a_{12}a_{21}a_{58}a_{85} + 4a_{17}a_{68}a_{76}a_{81} - 4a_{17}a_{31}a_{63}a_{76}}{T},$$
$$\beta_{18} = \frac{6a_{12}a_{21}a_{58}a_{85} + 6a_{17}a_{68}a_{76}a_{81} - 6a_{17}a_{31}a_{63}a_{76}}{T^2},$$
$$\beta_{19} = \frac{4a_{12}a_{21}a_{58}a_{85} + 4a_{17}a_{68}a_{76}a_{81} - 4a_{17}a_{31}a_{63}a_{76}}{T^3},$$
$$\beta_{20} = \frac{a_{12}a_{21}a_{58}a_{85} + a_{17}a_{68}a_{76}a_{81} - a_{17}a_{31}a_{63}a_{76}}{T^4},$$
$$\beta_{21} = a_{17}a_{41}a_{54}a_{65}a_{76} - a_{17}a_{58}a_{65}a_{76}a_{81},$$
$$\beta_{22} = \frac{3a_{17}a_{41}a_{54}a_{65}a_{76} - 3a_{17}a_{58}a_{65}a_{76}a_{81}}{T},$$
$$\beta_{23} = \frac{3a_{17}a_{41}a_{54}a_{65}a_{76} - 3a_{17}a_{58}a_{65}a_{76}a_{81}}{T^2},$$
$$\beta_{24} = \frac{a_{17}a_{41}a_{54}a_{65}a_{76} - a_{17}a_{58}a_{65}a_{76}a_{81}}{T^3};$$

$$d_1 = \cos 4\pi, \quad d_2 = \beta_1 \cos\frac{7\alpha\pi}{2}, \quad d_3 = \beta_2 \cos 3\pi,$$
$$d_4 = \beta_3 \cos\frac{5\alpha\pi}{2}, \quad d_5 = \beta_4 \cos 2\pi, \quad d_6 = \beta_5 \cos\frac{3\alpha\pi}{2},$$
$$d_7 = \beta_6 \cos\pi, \quad d_8 = \beta_7 \cos\frac{\alpha\pi}{2}, \quad d_9 = \beta_8,$$
$$d_{10} = \sin 4\pi, \quad d_{11} = \beta_1 \sin\frac{7\alpha\pi}{2}, \quad d_{12} = \beta_2 \sin 3\pi,$$
$$d_{13} = \beta_3 \sin\frac{5\alpha\pi}{2}, \quad d_{14} = \beta_4 \sin 2\pi, \quad d_{15} = \beta_5 \sin\frac{3\alpha\pi}{2},$$
$$d_{16} = \beta_6 \sin\pi, \quad d_{17} = \beta_7 \sin\frac{\alpha\pi}{2}, \quad d_{18} = \beta_9 \cos 3\pi,$$
$$d_{19} = \beta_{10} \cos\frac{5\alpha\pi}{2}, \quad d_{20} = \beta_{11} \cos 2\pi, \quad d_{21} = \beta_{12} \cos\frac{3\alpha\pi}{2},$$
$$d_{22} = \beta_{13} \cos\pi, \quad d_{23} = \beta_{14} \cos\frac{\alpha\pi}{2}, \quad d_{24} = \beta_{15},$$
$$d_{25} = \beta_9 \sin 3\pi, \quad d_{26} = \beta_{10} \sin\frac{5\alpha\pi}{2}, \quad d_{27} = \beta_{11} \sin 2\pi,$$
$$d_{28} = \beta_{12} \sin\frac{3\alpha\pi}{2}, \quad d_{29} = \beta_{13} \sin\pi, \quad d_{30} = \beta_{14} \sin\frac{\alpha\pi}{2},$$
$$d_{31} = \beta_{16} \cos 2\pi, \quad d_{32} = \beta_{17} \cos\frac{3\alpha\pi}{2}, \quad d_{33} = \beta_{18} \cos\pi,$$
$$d_{34} = \beta_{19} \cos\frac{\alpha\pi}{2}, \quad d_{35} = \beta_{20}, \quad d_{36} = \beta_{16} \sin 2\pi,$$

$$d_{37} = \beta_{17} \sin \frac{3\alpha\pi}{2}, \quad d_{38} = \beta_{18} \sin \pi, \quad d_{39} = \beta_{19} \sin \frac{\alpha\pi}{2},$$
$$d_{40} = \beta_{21} \cos \frac{3\alpha\pi}{2}, \quad d_{41} = \beta_{22} \cos \pi, \quad d_{42} = \beta_{23} \cos \frac{\alpha\pi}{2},$$
$$d_{43} = \beta_{24}, \quad d_{44} = \beta_{21} \sin \frac{3\alpha\pi}{2}, \quad d_{45} = \beta_{22} \sin \pi,$$
$$d_{46} = \beta_{23} \sin \frac{\alpha\pi}{2}.$$

References

1. Y. Chang, Y. Pei, R. Ponce, Existence and optimal controls for fractional stochastic evolution equations of Sobolev type via fractional resolvent operators, *J. Optim. Theory Appl.*, **182**:558–572, 2019, https://doi.org/10.1007/s10957-018-1314-5.
2. Y. Chang, Y. Wei, Pseudo S-asymptotically Bloch type periodic solutions to fractional integro-differential equations with Stepanov-like force terms, *Z. Angew. Math. Phys.*, **73**:77, 2022, https://doi.org/10.1007/s00033-022-01722-y.
3. G. Chen, Y. Zheng, D. Yi, Q. Zeng, Oscillation dynamics analysis of Parkinson's model with time delay, *Chin. J. Theor. Appl. Mech.*, **54**(10):2874–2882, 2022, https://doi.org/10.6052/0459-1879-22-307.
4. R. Chen, P.C. Chaparro-Pedraza, S. Xiao, A.M. de Roos, Marine reserves promote cycles in fish populations on ecological and evolutionary time scales, *Proc. Natl. Acad. Sci.*, **120**(47): e2307529120, 2023, https://doi.org/10.1073/pnas.2307529120.
5. J. Cousineau, V. Plateau, J. Baufreton, M. Le Bon-Jégo, Dopaminergic modulation of primary motor cortex: From cellular and synaptic mechanisms underlying motor learning to cognitive symptoms in Parkinson's disease, *Neurobiol. Dis.*, **167**:105674, 2022, https://doi.org/10.1016/j.nbd.2022.105674.
6. L. Guo, L. Liu, Maximal and minimal iterative positive solutions for singular infinite-point p-Laplacian fractional differential equations, *Nonlinear Anal. Model. Control*, **23**(6):851–865, 2018, https://doi.org/10.15388/NA.2018.6.3.
7. L. Guo, L. Liu, Y. Wu, Iterative unique positive solutions for singular p-Laplacian fractional differential equation system with several parameters, *Nonlinear Anal. Model. Control*, **23**(2): 182–203, 2018, https://doi.org/10.15388/NA.2018.2.3.
8. L.-M. Guo, J.-W. Cai, Z.-Y. Xie, C. Li, Mechanical responses of symmetric straight and curved composite microbeams, *J. Vib. Eng. Technol.*, **12**(2):1537–1549, 2024, https://doi.org/10.1007/s42417-023-00924-6.
9. C. Hammond, H. Bergman, P. Brown, Pathological synchronization in Parkinson's disease: Networks, models and treatments, *Trends Neurosci.*, **30**(7):357–364, 2007, https://doi.org/10.1016/j.tins.2007.05.004.
10. J.K. Haumesser, M.H. Beck, F. Pellegrini, J. Kühn, W.-J. Neumann, J. Altschüler, D. Harnack, A. Kupsch, V.V. Nikulin, A.A. Kühn, C. van Riesen, Subthalamic beta oscillations correlate with dopaminergic degeneration in experimental parkinsonism, *Exp. Neurol.*, **335**:113513, 2021, https://doi.org/10.1016/j.expneurol.2020.113513.

11. J. Hirschmann, A. Steina, J. Vesper, E. Florin, A. Schnitzler, Neuronal oscillations predict deep brain stimulation outcome in Parkinson's disease, *Brain Stimul.*, **15**(3):792–802, 2022, https://doi.org/10.1016/j.brs.2022.05.008.

12. A.J.N. Holgado, J. Terry, R. Bogacz, Conditions for the generation of beta band activity in Parkinson's disease, *BMC Neurosci.*, **10**(1):247, 2009, https://doi.org/10.1186/1471-2202-10-S1-P247.

13. N. Huang, G. Wang, T. Guan, The dynamics analysis of a new wine fermentation model, *J. Appl. Math. Comput.*, **70**:3731–3747, 2024, https://doi.org/10.1007/s12190-024-02106-3.

14. H. Kerkache, H. Hoang, P. Cézac, S. Chabab, The solubility of H_2 in NaCl brine at high pressures and high temperatures: Molecular simulation study and thermodynamic modeling, *J. Mol. Liq.*, **400**:124497, 2024, https://doi.org/10.1016/j.molliq.2024.124497.

15. P. Li, J. Yan, C. Xu, Y. Shang, Dynamic analysis and bifurcation study on fractional-order tri-neuron neural networks incorporating delays, *Fractal Fract.*, **6**(3):161, 2022, https://doi.org/10.3390/fractalfract6030161.

16. S.A. Lindi, N.P. Mallet, A. Leblois, Synaptic changes in pallidostriatal circuits observed in the Parkinsonian model triggers abnormal beta synchrony with accurate spatio-temporal properties across the basal ganglia, *J. Neurosci.*, **44**(9):e0419232023, 2024, https://doi.org/10.1523/JNEUROSCI.0419-23.2023.

17. C. Liu, Y. Zhu, F. Liu, J. Wang, H. Li, B. Deng, C. Fietkiewicz, K.A. Loparo, Neural mass models describing possible origin of the excessive beta oscillations correlated with Parkinsonian state, *Neural Netw.*, **88**:65–73, 2017, https://doi.org/10.1016/j.neunet.2017.01.011.

18. F. Liu, J. Wang, C. Liu, H. Li, B. Deng, C. Fietkiewicz, K.A. Loparo, A neural mass model of basal ganglia nuclei simulates pathological beta rhythm in Parkinson's disease, *Chaos*, **26**(12):123113, 2016, https://doi.org/10.1063/1.4972200.

19. N. Liu, Y. Bi, H. Yang, Q. Liu, Analyses of oscillation dynamics in cortex-basal ganglia-thalamus network, *J. Dyn. Control*, **18**(1):76–81, 2020, https://doi.org/10.6052/1672-6553-2020-008.

20. A. Nambu, Y. Tachibana, Mechanism of parkinsonian neuronal oscillations in the primate basal ganglia: some considerations based on our recent work, *Front. Syst. Neurosci.*, **8**:74, 2014, https://doi.org/10.3389/fnsys.2014.00074.

21. A. Pavlides, S.J. Hogan, R. Bogacz, Computational models describing possible mechanisms for generation of excessive beta oscillations in Parkinson's disease, *PLoS Comput. Biol.*, **11**(12):e1004609, 2015, https://doi.org/10.1371/journal.pcbi.1004609.

22. K. Shah, T. Abdeljawad, A. Ali, Mathematical analysis of the Cauchy type dynamical system under piecewise equations with Caputo fractional derivative, *Chaos Solitons Fractals*, **161**:112356, 2022, https://doi.org/10.1016/j.chaos.2022.112356.

23. J. Shi, K. He, H. Fang, Chaos, Hopf bifurcation and control of a fractional-order delay financial system, *Math. Comput. Simul.*, **194**:348–364, 2022, https://doi.org/10.1016/j.matcom.2021.12.009.

24. D.J. Surmeier, J. Ding, M. Day, Z. Wang, W. Shen, D_1 and D_2 dopamine-receptor modulation of striatal glutamatergic signaling in striatal medium spiny neurons, *Trends Neurosci.*, **30**(5): 228–235, 2007, https://doi.org/10.1016/j.tins.2007.03.008.

25. G. Wang, X. Ren, Z. Bai, W. Hou, Radial symmetry of standing waves for nonlinear fractional Hardy–Schrödinger equation, *Appl. Math. Lett.*, **96**:131–137, 2019, https://doi.org/10.1016/j.aml.2019.04.024.

26. G. Wang, R. Yang, L. Zhang, The properties of a new fractional g-Laplacian Monge–Ampère operator and its applications, *Adv. Nonlinear Anal.*, **13**(1):20240031, 2024, https://doi.org/10.1515/anona-2024-0031.

27. Z. Wang, M. Du, M. Shi, Stability test of fractional delay systems via integration, *Sci. China Phys., Mech. Astron.*, **54**:1839–1846, 2011, https://doi.org/10.1007/s11433-011-4447-1.

28. Z. Wang, X. Huang, H. Shen, Control of an uncertain fractional order economic system via adaptive sliding mode, *Neurocomputing*, **83**:83–88, 2012, https://doi.org/10.1016/j.neucom.2011.11.018.

29. T. Wichmann, M.R. DeLong, J. Guridi, A. Obeso, Milestones in research on the pathophysiology of Parkinson's disease, *Movement Disord.*, **26**(6):103, 2011, https://doi.org/10.1002/mds.23695.

30. Q. Zeng, Y. Zheng, D. Yi, Bifurcation analysis of a Parkinson's disease model with two time delays, *Math. Comput. Simul.*, **219**:1–11, 2024, https://doi.org/10.1016/j.matcom.2023.12.007.

31. L. Zhang, B. Ahmad, G. Wang, X. Ren, Radial symmetry of solution for fractional p-Laplacian system, *Nonlinear Anal., Theory Methods Appl.*, **196**:111801, 2020, https://doi.org/10.1016/j.na.2020.111801.

32. L. Zhang, W. Hou, Standing waves of nonlinear fractional p-Laplacian Schrödinger equation involving logarithmic nonlinearity, *Appl. Math. Lett.*, **102**:106149, 2020, https://doi.org/10.1016/j.aml.2019.106149.

33. L. Zhang, Q. Liu, B. Ahmad, G. Wang, Nonnegative solutions of a coupled k-Hessian system involving different fractional Laplacians, *Fract. Calc. Appl. Anal.*, **27**:1835–1851, 2024, https://doi.org/10.1007/s13540-024-00277-1.

34. L. Zhang, K. Lu, G. Wang, An efficient numerical method based on Chelyshkov operation matrix for solving a type of time-space fractional reaction diffusion equation, *J. Appl. Math. Comput.*, **70**:351–374, 2024, https://doi.org/10.1007/s12190-023-01971-8.

35. X. Zhang, L. Liu, Y. Wu, B. Wiwatanapataphee, Nontrivial solutions for a fractional advection dispersion equation in anomalous diffusion, *Appl. Math. Lett.*, **66**:1–8, 2017, https://doi.org/10.1016/j.aml.2016.10.015.